NeuroImage: Clinical 36 (2022) 103151

Contents lists available at ScienceDirect

NeuroImage: Clinical

journal homepage: www.elsevier.com/locate/ynicl

A diffusion MRI study of brain white matter microstructure in adolescents and adults with a Fontan circulation: Investigating associations with resting and peak exercise oxygen saturations and cognition

Charlotte E Verrall [a,b], Jian Chen [c], Chun-Hung Yeh [d], Mark T Mackay [e,f,g], Yves d'Udekem [h], David S Winlaw [i], Ajay Iyengar [j,k], Julian Ayer [a,b], Thomas L Gentles [j], Rachael Cordina [b,l], Joseph Y-M Yang [c,f,g,m,*]

[a] Heart Centre for Children, The Children's Hospital at Westmead, Sydney, Australia
[b] Sydney Medical School, Faculty of Medicine and Health, University of Sydney, Sydney, Australia
[c] Developmental Imaging, Murdoch Children's Research Institute, Melbourne, Australia
[d] Institute for Radiological Research, Chang Gung University, Taoyuan, Taiwan
[e] Department of Neurology, The Royal Children's Hospital, Melbourne, Australia
[f] Neuroscience Research, Murdoch Children's Research Institute, Melbourne, Australia
[g] Department of Paediatrics, University of Melbourne, Melbourne, Australia
[h] The Division of Cardiovascular Surgery, Children's National Heart Institute, Washington, DC, USA
[i] Cardiothoracic Surgery, The Heart Institute, Cincinnati Children's Hospital Medical Center, Cincinnati, OH, USA
[j] Green Lane Paediatric and Congenital Cardiac Service, Starship Children's Health, Auckland, New Zealand
[k] Department of Surgery, University of Auckland, Auckland, New Zealand
[l] Department of Cardiology, Royal Prince Alfred Hospital, Sydney, Australia
[m] Department of Neurosurgery, Neuroscience Advanced Clinical Imaging Service (NACIS), Royal Children's Hospital, Melbourne, Australia

ARTICLE INFO

Keywords:
White matter microstructure
Diffusion brain magnetic resonance imaging
Fontan circulation
Cognition

ABSTRACT

Introduction: Adolescents and adults with a Fontan circulation are at risk of cognitive dysfunction; Attention and processing speed are notable areas of concern. Underlying mechanisms and brain alterations associated with worse long-term cognitive outcomes are not well determined. This study investigated brain white matter microstructure in adolescents and adults with a Fontan circulation and associations with resting and peak exercise oxygen saturations (SaO_2), predicted maximal oxygen uptake during exercise (% pred VO_2), and attention and processing speed.

Methods: Ninety-two participants with a Fontan circulation (aged 13–49 years, ≥5 years post-Fontan completion) had diffusion MRI. Averaged tract-wise diffusion tensor imaging (DTI) metrics were generated for 34 white matter tracts of interest. Resting and peak exercise SaO_2 and % pred VO_2 were measured during cardiopulmonary exercise testing (CPET; N = 81). Attention and processing speed were assessed using Cogstate (N = 67 and 70, respectively). Linear regression analyses adjusted for age, sex, and intracranial volume were performed to investigate associations between i) tract-specific DTI metrics and CPET variables, and ii) tract-specific DTI metrics and attention and processing speed z-scores.

Results: Forty-nine participants were male (53%), mean age was 23.1 years (standard deviation (SD) = 7.8 years). Mean resting and peak exercise SaO_2 were 93.1% (SD = 3.6) and 90.1% (SD = 4.7), respectively. Mean attention

Abbreviations: AD, axial diffusivity; AF, arcuate fasciculus; ATR, anterior thalamic radiation; CC, corpus callosum; CG, cingulum; CHD, congenital heart disease; CHW, The Children's Hospital at Westmead; CSD, Constrained Spherical Deconvolution; CSF, cerebrospinal fluid; CST, corticospinal tract; CPET, cardiopulmonary exercise testing; dMRI, Diffusion Magnetic Resonance Imaging; DTI, Diffusion Tensor Imaging; DWI, Diffusion Weighted Imaging; FA, fractional anisotropy; FOD, fiber orientation distribution; FPT, frontopontine tract; GM, gray matter; GMCT, Groton Maze Chase test; HARDI, High Angular Resolution Diffusion Imaging; ICP, inferior cerebellar peduncle; ICV, intracranial volume; IFO, inferior fronto-occipital fasciculus; ILF, inferior longitudinal fasciculus; MCP, middle cerebellar peduncle; MD, mean diffusivity; MRI, Magnetic Resonance Imaging; RCH, Royal Children's Hospital; RPAH, Royal Prince Alfred Hospital; RD, radial diffusivity; SaO_2, oxygen saturations; SCP, superior cerebellar peduncle; SLF, superior longitudinal fasciculus (components I, II, and III); TOI, tracts of interest; WM, white matter; UF, uncinate fasciculus; % pred VO_2, predicted maximal oxygen uptake during exercise.

* Corresponding author at: Department of Neurosurgery, Royal Children's Hospital, Melbourne 3052, Australia.
E-mail address: joseph.yang4@rch.org.au (J. Y-M Yang).

https://doi.org/10.1016/j.nicl.2022.103151
Received 1 May 2022; Received in revised form 9 August 2022; Accepted 10 August 2022
Available online 12 August 2022

and processing speed z-scores were −0.63 (SD = 1.07) and −0.72 (SD = 1.44), respectively. Resting SaO_2 were positively associated with mean fractional anisotropy (FA) of the left corticospinal tract (CST) and right superior longitudinal fasciculus I (SLF-I) and negatively associated with mean diffusivity (MD) and radial diffusivity (RD) of the right SLF-I ($p \leq 0.01$). Peak exercise SaO_2 were positively associated with mean FA of the left CST and were negatively associated with mean RD of the left CST, MD of the left frontopontine tract, MD, RD and axial diffusivity (AD) of the right SLF-I, RD of the left SLF-II, MD, RD and AD of the right SLF-II, and MD and RD of the right SLF–III ($p \leq 0.01$). Percent predicted VO_2 was positively associated with FA of the left uncinate fasciculus ($p < 0.01$). Negative associations were identified between mean FA of the right arcuate fasciculus, right SLF-II and right SLF-III and processing speed ($p \leq 0.01$). No significant associations were identified between DTI-based metrics and attention.

Conclusion: Chronic hypoxemia may have long-term detrimental impact on white matter microstructure in people living with a Fontan circulation. Paradoxical associations between processing speed and tract-specific DTI metrics could be suggestive of compensatory white matter remodeling. Longitudinal investigations focused on the mechanisms and trajectory of altered white matter microstructure and associated cognitive dysfunction in people with a Fontan circulation are required to better understand causal associations.

1. Introduction

Neurodevelopmental delay and cognitive dysfunction are among the most common comorbidities in children living with a Fontan circulation and are associated with altered brain development and growth (Marelli et al., 2016; Verrall et al., 2019). Advances in perioperative and clinical care have dramatically improved survival and the number of adults living with a Fontan circulation now surpasses that of children (Plappert et al., 2022; d'Udekem et al., 2014), however, cognitive dysfunction is a concern throughout the life course.

We recently demonstrated significant cognitive impairments in an older Fontan population that included adolescents and adults (aged 13–49 years). Worse neurological and cognitive outcomes were identified in the adult Fontan cohort, suggestive of continued pathophysiological alterations in the brain of Fontan subjects as they age (Verrall et al., 2021). Cognitive impairments of particular concern included attention and reduced processing speed that impacted one-third of our cohort, with 16% and 13% demonstrating severe dysfunction in these domains, respectively. Similar findings have been demonstrated in other adolescent and adult complex congenital heart disease (CHD) cohorts, with an increased risk of dysfunction associated with CHD complexity (Klouda et al., 2017; Mills et al., 2018). These cognitive functions are foundational for other 'higher-order' cognitive abilities, such as executive functioning and memory (Harvey, 2019), that are also frequently reported domains of dysfunction in adolescents and adults with complex CHD (Verrall et al., 2021; Cassidy et al., 2015; Bellinger et al., 2015; Cabrera-Mino et al., 2020). Symptoms of attention deficit hyperactivity disorder are increased in individuals with a Fontan circulation (Hansen et al., 2012) and commonly emerge during adolescence alongside increasing educational demands and independent functioning. Fluid abilities such as processing speed and attention are most susceptible to age-related decline in typically developing populations. Consistent with the increased risk of dementia in adults with CHD (Bagge et al., 2018), our previous findings suggest possible accelerated cognitive decline in adults with a Fontan circulation (Verrall et al., 2021).

Fontan physiology is characterized by unique hemodynamics, including prolonged mild cyanosis that often results from a patent fenestration (allowing right to left shunting of deoxygenated blood to the systemic circulation) and development of veno-venous collaterals or pulmonary arteriovenous malformations (Ohuchi, 2017). Reduced exercise tolerance is also a concern and may have important functional implications (Tran et al., 2022). Chronic hypoxemia is associated with long-term morbidity and late mortality, even in cases of mild desaturation (Schafstedde et al., 2021; Egbe et al., 2017; Zentner et al., 2020), and may be an important predisposing factor for altered cerebral development, white matter (WM) injury, and subsequent cognitive functioning (Owen et al., 2011; Morton et al., 2017; Limperopoulos et al., 2010; Sun et al., 2015; Claessens et al., 2018; Spaeder et al., 2017; Claessens et al., 2019; Rajagopalan et al., 2018; Lee et al., 2021; Sadhwani et al., 2022). Significant reductions in global brain volume and subcortical gray matter (GM) volume were associated with lower SaO_2 in our adolescent and adult Fontan cohort (Verrall et al., 2021), consistent with our earlier findings from adults with other forms of cyanotic CHD (Cordina et al., 2014). Smaller global brain volumes were associated with worse cognitive outcomes in our Fontan cohort (Verrall et al., 2021), and other older CHD cohorts (Naef et al., 2021; von Rhein et al., 2014). Importantly, associations between hypoxemia and WM microstructure in people with a Fontan circulation and subsequent cognitive impairment have not yet been established.

Diffusion MRI (dMRI) is the preferred neuroimaging technique to visualise brain WM tracts, and to study changes in WM microstructural properties and network organization associated with brain development, aging, and a variety of neurological disorders (Yang et al., 2021; Tamnes and Agartz, 2016). Diffusion tensor imaging (DTI) (Basser et al., 1994; Basser et al., 1994), the simplest diffusion WM model, and its quantitative metrics, have been used as imaging surrogates to infer WM microstructural injuries in children and adolescents with complex CHD (Rivkin et al., 2013; Rollins et al., 2014; Watson et al., 2018; Brewster et al., 2015; Singh et al., 2019). Demyelination or axonal injury can be suggested by a DTI metrics pattern of reduced fractional anisotropy (FA) and increased mean diffusivity (MD) (Alexander et al., 2007); such alterations were shown to be associated with worse cognitive functioning (Rollins et al., 2014; Watson et al., 2018; Brewster et al., 2015; Singh et al., 2019). Altered WM microstructure in varying WM tracts has been reported in young adults with complex CHD (Ehrler et al., 2020), with notable implications for executive functioning (Ehrler et al., 2021). Associations between WM microstructure and cognitive functioning in a Fontan-specific cohort, that is inclusive of adolescents, young- and middle-aged adults, have not been investigated.

This exploratory study aimed to i) investigate associations between resting and peak exercise SaO_2 and predicted maximal oxygen uptake during exercise (% pred VO_2) and WM tract-specific DTI metrics in adolescents and adults with a Fontan circulation and ii) explore the associations between these tract-specific DTI metrics, as surrogates of WM microstructural properties, with attention and processing speed.

2. Methods

2.1. Participants

Full recruitment details have previously been described elsewhere (Verrall et al., 2021). All participants were recruited as part of the broader Fontan Registry 'Functional Outcomes after Fontan Surgery' study between April 2015 and November 2018, participation occurred at the Royal Children's Hospital (RCH; Melbourne), The Children's Hospital at Westmead and Royal Prince Alfred Hospital (CHW and RPAH; Sydney), and Starship Children's Hospital (Starship; Auckland). Inclusion criteria included individuals with a Fontan circulation who

were between 13 and 49 years of age, ≥5 years post-Fontan completion and who were enrolled in the Australian and New Zealand Fontan Registry. Exclusion criteria included contraindication to undergo MRI and/or an existing diagnosis of severe intellectual disability or a clinically diagnosed genetic syndrome associated with cognitive impairment identified from their medical record. Ethics approval was granted at each site and written informed consent was obtained from all participants.

2.2. Clinical and cognitive assessment

Resting and peak exercise arterial SaO_2 and % pred VO_2 were measured during cardiopulmonary exercise testing (CPET) and were included as measures of hypoxemia and related exercise tolerance, respectively. Clinical data were collected from existing records in the Australia and New Zealand Fontan Registry and from patients' medical records at their treating hospitals by trained database managers.

Attention and processing speed were included as cognitive functions of interest as our previous results demonstrated the greatest incidence of severe impairment in these domains. These functions were assessed using Cogstate, a validated, culture-neutral computerised assessment program (Maruff et al., 2009; Hammers et al., 2012). The Groton Maze Chase test (GMCT) is a visual measure of processing speed requiring the subject to chase a moving target through a maze as quickly as possible. The Identification test (IDN) is a measure of sustained attention that uses a choice reaction paradigm whereby the subject needs to identify whether a playing card is red by clicking "yes" or "no" as quickly as possible after a card is presented on screen. Participants completed the assessment onsite at the participating hospitals. A short pre-test practice was provided prior to each test for participants to familiarise themselves with the instructions. Raw scores underwent an automated integrity test to measure whether performance was in accordance with test requirements, all test integrity fail scores, or completion fail scores were excluded from the analysis. Raw scores were standardized to z-scores using Cogstate pediatric and adult age normative data, and then transformed so that lower scores were indicative of poorer performance.

2.3. MRI data acquisition

Brain MRI was performed using Siemens 3Tesla MRI scanners; RCH (TrioTim), RPAH (Skyra), CHW (Verio), and Starship (Skyra). Acquisition included a 3D MPRAGE T1-weighted imaging sequence at 0.8–0.9 mm isotropic voxel resolution, and a High Angular Resolution Diffusion Imaging (HARDI) sequence based on the twice-refocused spin-echo diffusion echo-planar imaging ($b = 3000$ s/mm^2; 60–64 noncolinear diffusion direction, 1–8b $= 0$ s/mm^2 volumes; 2.3–2.4 mm isotropic voxel resolution). Of the original cohort ($n = 102$) who had Diffusion-Weighted Imaging (DWI), eight cases with notable distorted brain structural anatomy related to post-stroke cerebral encephalomalacia and cerebral gliosis were excluded. Processing of their MRI data would likely lead to complete or partial failure of tractography reconstructions (see tractography method below). Two additional cases were excluded due to suboptimal DWI quality relating to motion artifacts. The DWI acquisition details from the four participating sites are summarized in the supplemental materials.

2.4. Data processing

Per-subject DWIs were processed using a combination of the software packages including MRtrix3 (version 3.160 RC3, *https://www.mrtrix.org/*) (Tournier et al., 2019), FSL, BrainSuite (*https://brainsuite.org*), ANTs, and TractSeg (Wasserthal et al., 2018) in the following subsections. To avoid the variances introduced by the inconsistencies in data acquisition within the RPAH site, we used only the data acquired at *b*-value $= 3000$ s/mm^2.

2.4.1. DWI pre-processing

The DWI data were pre-processed sequentially to correct for: data thermal noise (Veraart et al., 2016); Gibbs-ringing artifacts (Kellner et al., 2016); *EPI* susceptibility-induced geometric distortions (Bhushan et al., 2015); eddy current and motion-induced distortions (Andersson et al., 2003; Andersson and Sotiropoulos, 2016); and *b1*-bias field induced inhomogeneity (Tustison et al., 2010).

2.4.2. WM tract segmentation and tractography

Tissue-specific response functions for WM, GM, and cerebrospinal fluid (CSF) were first estimated using an unsupervised single-shell three-tissue response function estimation algorithm (Dhollander et al., 2016) for each individual. Voxel-wise fiber orientation distributions (FODs) were computed based on individual's WM and CSF response functions and the multi-tissue constrained spherical deconvolution (CSD) to estimate the WM-FOD and CSF compartment (Jeurissen et al., 2014); $l_{max} = 8$. Seventy-two WM tracts were reconstructed from each DWI dataset using TractSeg, an automated WM tract segmentation technique. TractSeg predicts the probability of WM tract from the provided WM FOD peaks, through a deep-learning algorithm (Wasserthal et al., 2018). To minimize the partial volume effect that includes GM and CSF compartments in the selected WM voxels, the TractSeg tract masks were further refined by confining to only the WM voxels for analysis (see Supplementary Document 1 for further details).

2.4.3. Tract-specific diffusion quantitative metrics

Thirty-four out of the 72 segmented WM tracts were selected as tracts of interest (TOI) in the current study analysis (Fig. 1). The selection criteria were determined based on previously reported associations between DTI metrics and processing speed and/or attention in people with CHD, including individuals with a Fontan circulation, and other clinical populations and healthy individuals (Watson et al., 2018; Brewster et al., 2015; Sasson et al., 2013;7:32–; Chiang et al., 2020; Cremers et al., 2016). The TOI included: bilateral association tracts (arcuate fasciculus (AF), cingulum, inferior fronto-occipital fasciculus (IFO), inferior longitudinal fasciculus (ILF), superior longitudinal fasciculus (SLF; components I, II, and III; hereinafter SLF-I, SLF-II, and SLF-III), and uncinate fasciculus (UF)), bilateral projection tracts (anterior thalamic radiation (ATR), corticospinal tract (CST), and fronto-pontine tract (FPT)), the corpus callosum (CC; 7 divisions based on the Witelson's classification (Witelson, 1989), and the brainstem tracts (bilateral superior and inferior cerebellar peduncle (SCP and ICP, respectively) and the middle cerebellar peduncle (MCP)).

The diffusion tensor was computed using the iterative weighted linear least square estimator (Basser et al., 1994; Veraart et al., 2013). The following averaged tract-specific DTI metrics were then derived from the respective diffusion scalar maps, within each tract mask: FA, MD, axial diffusivity (AD) and radial diffusivity (RD).

2.4.4. Data harmonization

To account for the multi-site, inter-scanner variances on the derived diffusion metrics, ComBat, a batch-effect correction method, was applied to all tract-wise DTI metrics, prior to the statistical analysis below (Fortin et al., 2017). Prior to data harmonization, we found that some DTI metrics were biased by acquisition protocol and site effect; ComBat adjustment effectively removed all significant site variability.

2.5. Statistical analysis

Data were analysed using SPSS version 28 (IBM Corp) and R software version 4.1.2 (R Foundation). Independent sample t-tests were performed to investigate differences in dMRI data between i) participants that had available CPET data compared to those that did not, and ii) participants that had attention and processing speed results compared to those that did not. Linear regression analyses adjusted for age, sex, and intracranial volume (ICV) were performed to investigate associations

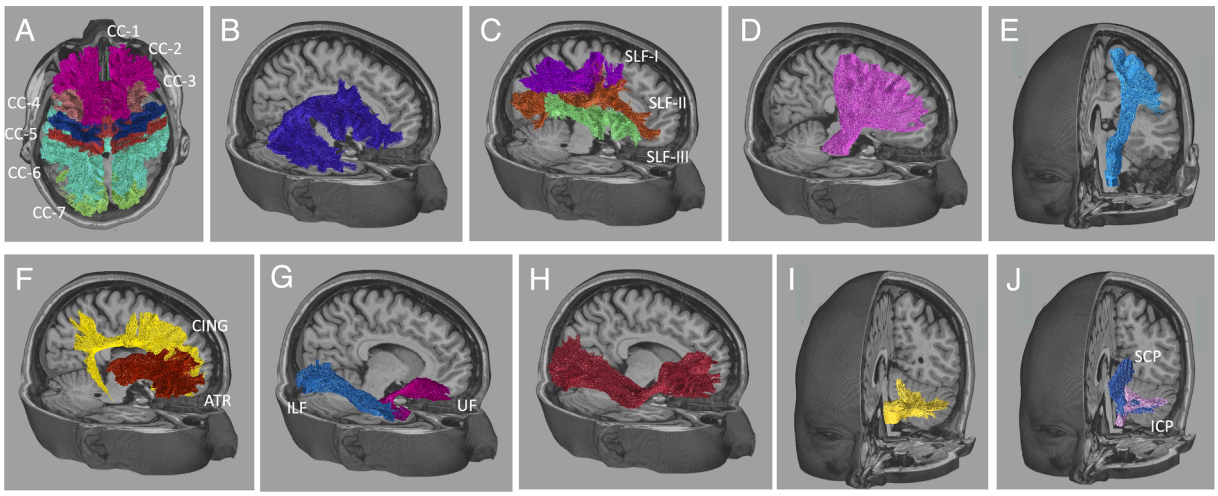

Fig. 1. Selected white matter tracts of interest in this study. **A:** 7 divisions of the corpus callosum (CC1-7) as per Witelson's classification, **B:** arcuate fasciculus, **C:** 3 components of the superior longitudinal fasciculus (SLF-I to III), **D:** fronto-pontine tract, **E:** corticospinal tract, **F:** cingulum (CING) and anterior thalamic radiation (ATR), **G:** inferior longitudinal fasciculus (ILF) and uncinate fasciculus (UF), **H:** inferior fronto-occipital fasciculus, **I:** middle cerebellar peduncle, **J:** superior cerebellar peduncle (SCP) and inferior cerebellar peduncle (ICP).

between i) CPET variables (i.e. resting and peak exercise SaO_2 and % pred VO_2; independent variables) and FA, MD, AD and RD of each TOI (dependant variables), and ii) FA, MD, AD and RD of each TOI (independent variables) and cognitive performance (i.e. attention and processing speed z-scores; dependant variables). A secondary analysis was performed that included an interaction term between age and the tract-specific DTI metrics in the linear regression models. A likelihood ratio test was also performed to compare the difference between the models with and without the interaction term. A secondary linear regression analysis adjusted for age, sex and ICV was performed to investigate associations between pre-Fontan SaO_2 and tract-specific DTI metrics. For all the analyses above, MD, AD and RD values were multiplied by 10,000 for reporting purposes. Bonferroni correction was applied to adjust for multiple comparisons (i.e. 0.05 divided by 4 (rounded to two decimal places), to adjust for the four DTI metrics included for each TOI) and a significance level of $p \leq 0.01$ was used to determine statistical significance.

3. Results

3.1. Cohort characteristics

From our original cohort (Verrall et al., 2021), 92/127 participants had dMRI and were included in the current study; 49 (53%) were male, mean age was 23.1 years (standard deviation (SD) = 7.8), clinical data for the current cohort are presented in Table 1. Of those, 81 participants had CPET. Mean resting and peak exercise SaO_2 were 93.1% (SD = 3.67) and 90.1% (SD = 4.71), respectively. Mean resting and peak exercise SaO_2 were significantly lower for those with a patent fenestration compared to those without ($p \leq 0.02$, see Supplementary Table 2). Sixty-seven participants had attention z-scores (mean = -0.63, SD = 1.07) and 70 had processing speed z-scores (mean = -0.72, SD = 1.44). Twenty participants did not complete the Cogstate assessment due to study limitations that would have required the participant to attend the hospital on a second occasion, the remaining missing data reflect failed test integrity or test completion (five and two participants, respectively). Mean FA, MD, AD and RD for each TOI are included in the Supplemental Materials (see Supplementary Table 3 and Supplementary Fig. 1). There were no significant differences in FA, MD, AD or RD between those that had CPET data, attention z-scores or processing speed z-scores and those that did not.

Table 1
Clinical characteristics.

Variables	
Age at Fontan, mean (SD)	6.08 (4.62)
Number of procedures prior to Fontan completion, n (%)	
0	2 (2%)
1	27 (29%)
2	35 (38%)
3	16 (17%)
4 or more	12 (13%)
Pre-Fontan SaO_2, mean (SD)*	82.3% (4.75)
Time since Fontan, mean (SD)	16.98 (6.54)
Primary diagnostic category, n (%)	
Hypoplastic left heart syndrome	8 (9%)
Pulmonary atresia with intact ventricular septum	10 (11%)
Pulmonary atresia with VSD	1 (1%)
Double inlet left ventricle	16 (17%)
Double outlet right ventricle	19 (21%)
Transposition of the great arteries	8 (9%)
Tricuspid atresia	20 (22%)
AVSD/atrioventricular canal	8 (9%)
Tetralogy of Fallot	1 (1%)
Aortic atresia	1 (1%)
Ventricular morphology, n (%)	
Left	55 (60%)
Right	25 (27%)
Biventricular	7 (8%)
Indeterminate	5 (5%)
Type of Fontan, n (%)	
Atriopulmonary	11 (12%)
Lateral tunnel	22 (24%)
Extracardiac conduit	57 (62%)
AP converted to extracardiac conduit	1 (1%)
Unknown	1 (1%)
Patent fenestration, n (%)	18 (20%)

*N = 70 due to some missing data; VSD = ventricular septal defect; AVSD = atrioventricular septal defect.

3.2. Oxygen saturations and tract-specific DTI metrics

Resting SaO_2 were positively associated with mean FA of the left CST (B = 0.002, [95% CI = 0 to 0.003], p = 0.01), and mean FA of the right SLF-I (B = 0.002, [0.001 to 0.004], p = 0.01) and negatively associated with mean MD and RD of the right SLF-I (B = -0.03, [-0.05 to −0.01], p = 0.01; B = -0.03, [-0.05 to −0.01], p = 0.01, respectively). Peak exercise SaO_2 were positively associated with mean FA of the left CST (B =

0.001, [0 to 0.003], p = 0.01) and were negatively associated with mean RD of the left CST (B = -0.01, [-0.02 to −0.004], p < 0.01), MD of the left FPT (B = -0.01, [-0.02 to −0.003], p = 0.01), MD, RD and AD of the right SLF-I (B = -0.04, [-0.06 to −0.02], p = 0.001; B = -0.04, [-0.06 to −0.01], p < 0.01; B = -0.03, [-0.05 to −0.01], p = 0.01, respectively), RD of the left SLF-II (B = -0.02, [-0.03 to −0.004], p = 0.01), MD, RD and AD of the right SLF-II (B = -0.02, [-0.03 to −0.01], p = 0.01; B = -0.02, [-0.03 to −0.004], p = 0.01; and B = -0.02, [-0.03 to −0.01], p = 0.01, respectively) and MD and RD of the right SLF-III (B = -0.01 [-0.02 to −0.003]. p = 0.01 and B = -0.01, [-0.03 to −0.003], p = 0.01, respectively); see Fig. 2 and Supplementary Tables 4 and 5. No significant age interaction effects were identified when this was included in the models, and no significant differences were demonstrated between the models with versus without the interaction term.

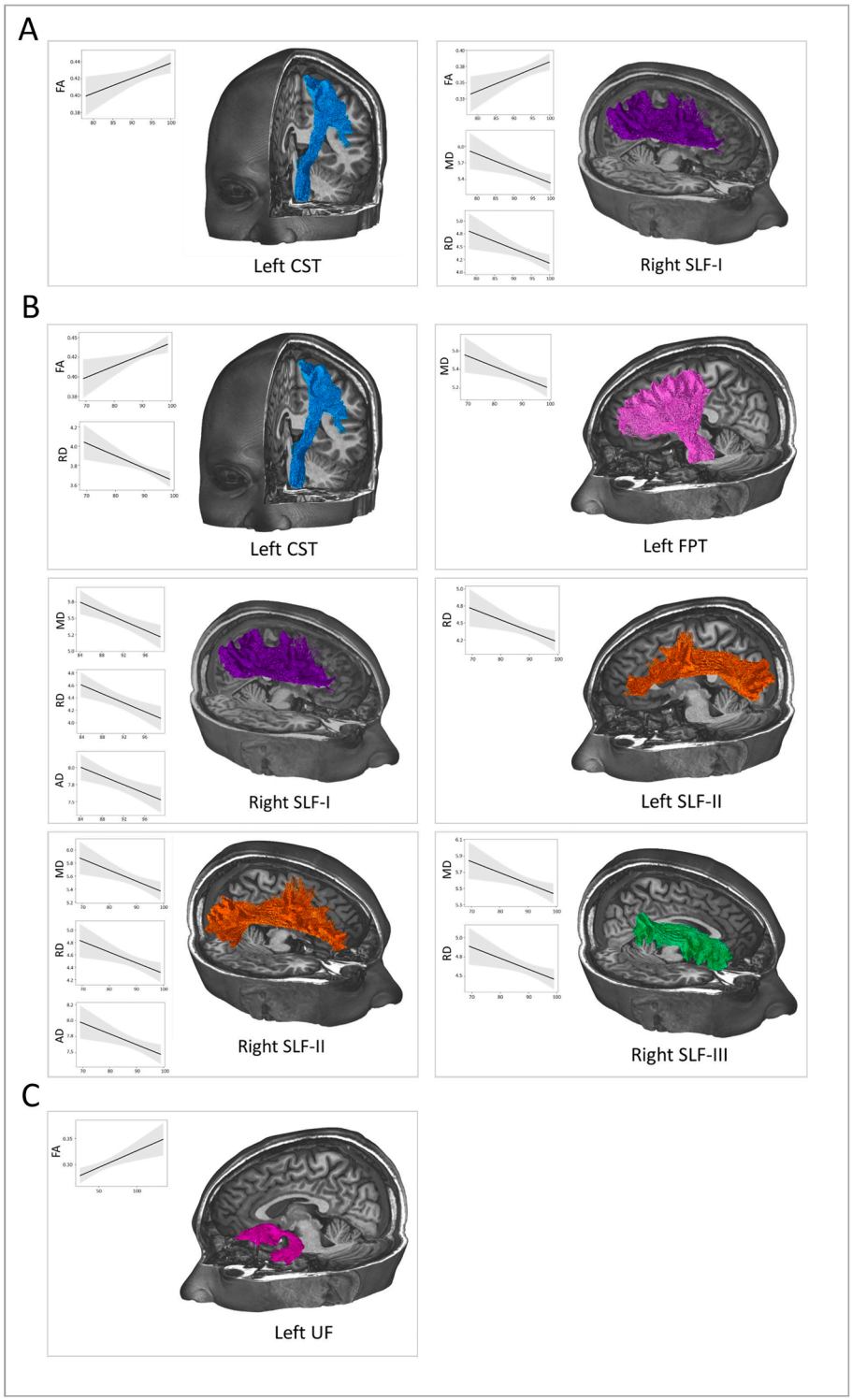

Fig. 2. Significant associations between resting and peak exercise oxygen saturations and tract-specific DTI metrics. **A:** Resting oxygen saturations, **B:** Peak exercise oxygen saturations, **C:** Percent predicted VO_2. FA = fractional anisotropy; MD = mean diffusivity; RD = radial diffusivity; AD = axial diffusivity; CST = corticospinal tract; FPT = fronto-pontine tract; SLF = superior longitudinal fasciculus (components I, II and III).

A significant positive association was identified between % pred VO_2 and mean FA of the left UF (B = 0.001, [0 to 0.001], p < 0.01). No significant associations were found between pre-Fontan SaO_2 and tract-specific DTId metrics.

3.3. Cognitive functioning and tract-specific DTI metrics

Significant associations were detected between mean FA of the right AF, right SLF-II and right SLF-III and processing speed whereby higher FA was associated with slower processing speed (B = -28.82, [-48.73 to −8.91], p < 0.01; B = -21.35 [-38.12 to −4.59], p = 0.01; and B = -21.21, [-37.95 to −4.47], p = 0.01, respectively), Fig. 3. No significant associations were identified between attention and tract-specific DTI metrics (see Supplementary Tables 6 and 7). No significant age interaction effects were identified when this was included in the models, and no significant differences were demonstrated between the models with versus without the interaction term.

No significant associations were identified between resting and peak exercise SaO_2 and attention or processing speed (Supplementary Table 8).

4. Discussion

The current findings demonstrate significant associations between resting and peak exercise SaO_2 and WM tract-specific DTI metrics in adolescents and adults with a Fontan circulation, whereby lower SaO_2 were associated with lower FA and higher MD, RD and/or AD in several long association and projection WM tracts, including the left CST, left FPT, right SLF-I and right SLF-III, and bilateral SLF-II. Lower % pred VO2 was associated with lower FA of the left UF.

Unexpectedly, processing speed was negatively associated with FA of the right SLF-II, right SLF-III and right AF, and no significant associations were identified between tract-specific DTI metrics and attention, suggesting that associations between DTI metrics and cognitive functioning may not have a uniform interpretation.

The current findings suggest that reduced SaO_2 during rest and in response to physical activity (thought to reflect persisting hypoxemia) could be a modifiable contributing factor to long-term alterations in WM microstructure in people with a Fontan circulation. These findings complement our earlier results demonstrating important associations between resting SaO_2 and brain volumetrics in people with a Fontan circulation (Verrall et al., 2021) and other complex CHD (Cordina et al., 2014). Reduced cerebral oxygen delivery *peri*-operatively has been associated with lower FA in children with complex CHD (Kelly et al., 2019) and smaller neonatal aorta size has been found to correlate with lower FA across multiple WM tracts during adolescence in people with Fontan physiology, suggesting perinatal cerebral blood flow may have a lasting impact on WM development in patients with a Fontan circulation (Zaidi et al., 2018). While oxygen saturations are corrected to near-normal levels at the time of Fontan completion for many children with single ventricle physiology, persisting hypoxemia occurs within varying severity for some individuals and may be associated with surgical factors. Fenestration of the Fontan circulation is performed in cases that are at increased risk for poor Fontan outcomes (Lemler et al., 2002) and may also be determined by institutional preferences. While fenestration may be beneficial in the early post-operative course, the presence of a patent fenestration is associated with long-term oxygen desaturation (Verrall et al., 2021) and greater desaturation during exercise (Heal et al., 2017) that may contribute to alterations in WM microstructure, however further investigation surrounding such associations is required beyond this current exploratory study. While we can only speculate on the mechanisms underlying the associations between lower oxygen saturations and WM microstructure, research in other clinical hypoxemic cohorts suggest that chronic hypoxia may be associated with demyelination and/or axonal injury (Issar et al., 2018; Martinez Sosa and Smith, 2017 Oct 12). It is possible that chronic hypoxemia may also impact myelin repair in response to persisting hypoxic-ischemic events (Cayre et al., 2021). Reduced SaO_2 in our cohort could be a surrogate for other issues including a small prenatal aortic arch, elevated central venous pressures, and/or low cardiac output (Ohuchi, 2017). Future longitudinal research including more detailed phenotyping is needed to determine causative associations. While pulse oximetry provides a non-invasive measure of SaO2, the collection of invasive hemodynamic data in future studies is justified and further research investigating associations with cardiorespiratory fitness are warranted.

Lower regional and tract-specific FA has been related to worse cognitive performance in recent adolescent CHD studies (Rollins et al., 2014). In a cohort of children and adolescents with a Fontan circulation, processing speed was significantly correlated with lower FA in the bilateral forceps minor and major, cerebral peduncle, IFO and ILF, as well as left CST and right external capsule, but these correlations were not identified in control subjects (Watson et al., 2018). Ehrler and colleagues recently demonstrated significant associations between worse executive function performance and reduced FA in the left superior corona radiata and left CST in emerging adults with complex CHD (aged 18–32 years) (Ehrler et al., 2021). In another young adult CHD cohort, a positive correlation between FA of the MCP and better auditory attention span has been demonstrated (Brewster et al., 2015).

In the current cohort inclusive of older adults with a Fontan circulation, counterintuitive associations were identified: FA correlated negatively with processing speed of the right SLF-II, right SLF-III and right AF, whereas there were no significant associations between tract-wise averaged DTI metrics and attention. The SLF-II, SLF-III, and AF contain long-range fronto-parietal and fronto-temporal association fibers that share a close anatomical location. In the right hemisphere, these tracts connect key cortical regions involved in visuospatial information and visuomotor processing with frontal areas involved in attentional allocation (Barbeau et al., 2020; Nakajima et al., 2020). In normally developing and other clinical cohorts, the FA values of the SLF were reported to be positively associated with processing speed (Jeurissen et al., 2014; McKenna et al., 2015). The GMCT task used to measure processing speed in our cohort is a visual measure, the efficient

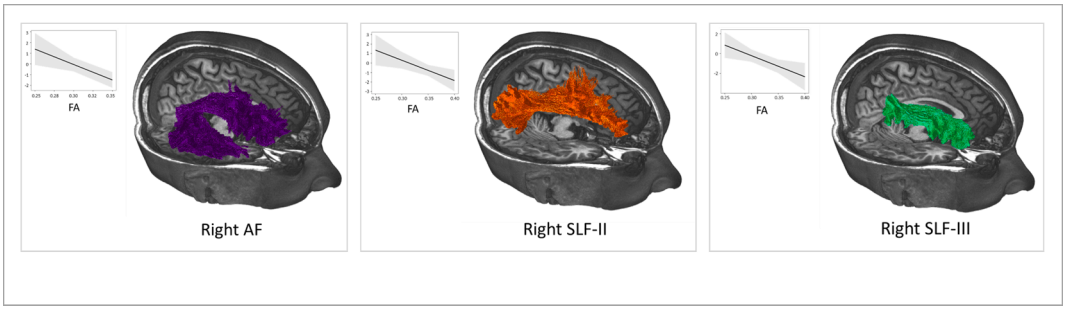

Fig. 3. Significant associations between tract-specific DTI metrics and processing speed. FA = fractional anisotropy; AF = arcuate fasciculus; SLF = superior longitudinal fasciculus (components II and III).

completion of which is dependent to an extent on visuospatial and visuomotor abilities, making this finding particularly unexpected. Hoeft and colleagues (2007) demonstrated similar paradoxical findings in a cohort of adults with Williams syndrome, whereby increased FA in the right SLF-II was significantly associated with worse visuospatial abilities (Hoeft et al., 2007). Counterintuitive associations between higher FA and worse cognitive functioning have also been identified in other clinical cohorts, including children and adolescents with autism spectrum disorder (Fitzgerald et al., 2015), and in people with schizophrenia despite lower mean FA compared to healthy controls (Jung et al., 2020; Kim et al., 2021). The inconsistent findings between the inferred WM microstructural properties and cognitive functioning in ours and other clinical cohorts suggests that the interpretation of these associations is not always uniform, and that higher FA does not always suggest improved cognitive functioning. Alterations in DTI metrics may reflect factors such as neuroinflammation, glial cell abnormalities and cerebral edema that can occur in response to hypoxic brain injury (Concha, 2014; Huang et al., 2014). Attention and processing speed are both considered to be complex neurobiological processes and it is also possible that tract-specific associations may be too simple to capture the complexity of neural networks involved in these functions (Penke et al., 2010). In addition, the interpretation of DTI metrics may be influenced by crossing fiber regions, particularly in the region of the centrum semiovale that includes the AF and SLF-I to -III (Groeschel et al., 2014).

It is postulated that the paradoxical associations between increased FA and worse cognitive functioning observed in other clinical cohorts might reflect compensatory but maladaptive, activity-dependent myelination that is not associated with restored cognitive functioning (Kim et al., 2021; Gibson et al., 2018). Although speculative and beyond the scope of this study, it is possible that aberrant WM remodelling and/or the engagement of compensatory neural circuits (Reuter-Lorenz and Park, 2014) may be occurring in response to early and persisting cognitive dysfunction and the accumulative burden of neurological injury across the lifespan of people with a Fontan circulation. Longitudinal data in healthy aging adults have shown that progressive reductions in FA have variable associations with processing speed despite significant associations at baseline assessment (Oschwald et al., 2019); highlighting between-person variability in cognitive deterioration that is likely reflective of cognitive reserve, that is an important vulnerability in adults with cyanotic CHD (Bagge et al., 2018). Longitudinal studies looking at the mechanisms and trajectory of WM alterations in conjunction with cognitive functioning in the older Fontan adult cohort are warranted to understand the pathophysiology underlying dysfunction in the aging Fontan population.

The interactive role of external and environmental factors should also be considered in future investigations and likely play a compounding factor in determining long-term cognitive outcomes. We previously demonstrated that geographical remoteness was significantly associated with executive functioning and visual learning in this cohort (Verrall et al., 2021). Length of ICU and post-operative hospital stay are considered key determinants of early- and medium-term neurodevelopment and cognition in children with complex CHD (Newburger et al., 2003), and sociodemographic factors such as maternal education and socioeconomic status have been associated with poorer developmental outcomes in children with single ventricle physiology (Bucholz et al., 2021). Educational and occupational achievements are hindered in some people with a Fontan circulation due to early cognitive difficulties, and challenges with socioemotional cognition has important implications for relationships and societal engagement. Combined, these outcomes contribute to poorer mental health and quality of life (Idorn et al., 2013). The accumulation of these challenges likely has a cyclical and exacerbating effect on long-term cognitive functioning, and moreover are possible modifiable factors that may promote more resilient cognitive reserve (Sattler et al., 2012).

Our selected imaging analytic strategy focused on WM tract specific measures that differ from a whole-brain voxel-based approach and tract-based spatial statistics methods that have been utilized in other DTI-based Fontan studies, which may account for some of the differences in our findings. In our study, additional steps were taken to minimize the partial volume effect, resulting in more WM specific diffusion metrics. We elected a multi-fiber WM model (i.e. multi-tissue CSD) as the basis to model the WM tract reconstructions (Jeurissen et al., 2014), overcoming the limitation of inaccurate WM tract mapping over crossing fiber regions, which is present in more than 70% of brain WM regions (Jeurissen et al., 2013).

We elected to use an automated tractography segmentation technique to ensure a standardized, data-driven tractography method is used, and to avoid potential tracking bias introduced by manual delineation of tracking regions-of-interest that is prone to high tracking variability (Schilling et al., 2021). The use of TractSeg does not explicitly account for the effect of brain pathology (Wasserthal et al., 2018), however, the included case cohorts contain WM microhemorrhage and small GM infarcts that do not result in significant anatomical distortion. The effects of these microscopic cerebral insults are likely able to be accounted for by the multi-tissue CSD, disentangling diffusion signal contributions by the different tissue-types presented in each dMRI voxel (Dhollander et al., 2016). Few cases with notable distorted brain anatomy, post-stroke cerebral encephalomalacia and gliotic changes were excluded prior to running TractSeg. Performance of TractSeg has also been previously evaluated using clinical grade dMRI data containing degrees of brain anatomy distortions, such as those with ventricular enlargement, and showed anatomically plausible results (Wasserthal et al., 2018).

4.1. Limitations

We selected the HARDI b = 3000 s/mm^2 data for the purpose of optimizing WM segmentation and tractography accuracy over the crossing fiber regions, but this could be suboptimal for DTI metrics estimation. Changes in DTI metrics can only be used as an indirect surrogate to infer WM microstructure injuries, as they are also subjected to alterations due to the effects of different neuropathological processes, such as chronic cerebral inflammation, and also by the crossing fiber axonal arrangements (Tournier et al., 2011; Tuch et al., 2002). The use of a more appropriate fiber-specific diffusion metric derived from a higher-order diffusion model is not applicable in this study due to the small sample size with heterogenous demographics from each participating site, and the lack of site-specific healthy, age-matched control data to establish effects of normal variance (Raffelt et al., 2017; Smith et al., 2020).

In a related point, ComBat, the data harmonization technique employed in this study for DTI metrics is well justified, given its effectiveness in reducing site variance had been previously demonstrated in large scale, multisite clinical cohort DTI studies (Hatton et al., 2020; Villalón-Reina et al., 2020) but its use for diffusion metrics derived from higher-order diffusion models had not been widely investigated. While multi-site MRI studies are frequently challenged for limitations surrounding scanner variability, the rarity of adult survivors with a Fontan circulation makes multi-site data-pooling beneficial to increase access to potential study participants.

Lastly, we elected to study selected TOI based on the functional role of the selected WM tracts described in the literature, thus enabled us to formulate appropriate a priori hypotheses. While we considered the tracts selected formulate a strong foundation for our exploratory analysis, an alternative approach would be to perform a network based analysis by reconstructing whole-brain structural connectome using the dMRI data, and to analyze connectome based metrics as surrogate to infer changes in WM microstructural properties and network organization (Yeh et al., 2021). However, such analysis scheme is not suited to the current multi-site dataset, including the lack of healthy controls as described previously. In addition, it was not appropriate to perform Bonferroni correction to account for the number of TOI included in this

exploratory analysis due to the sample size being underpowered, as such the current findings should be interpreted with caution.

5. Conclusions

Resting and peak exercise SaO_2 are associated with altered patterns of tract-specific DTI metrics in several key WM tracts in adolescents and adults with a Fontan circulation, suggesting that chronic hypoxemia may impact long-term brain WM microstructure. Future efforts to minimize persisting hypoxemia may be beneficial. Paradoxical associations were identified between tract-specific DTI metrics and processing speed that could reflect compensatory WM remodeling. Further investigations are required to understand the trajectory and mechanisms underlying altered WM microstructure in this cohort.

6. Data availability statement

The clinical and MRI data used in this study was acquired from clinical patients. They were not made openly available due to ethics issue of handling clinical data.

7. Disclosures

The authors declare no competing interests relevant to the manuscript. Dr Joseph Yuan-Mou Yang receives positional funding from the Royal Children's Hospital Foundation (RCH 1000).

CRediT authorship contribution statement

Charlotte E Verrall: Conceptualization, Methodology, Software, Formal analysis, Investigation, Data curation, Writing – original draft, Visualization, Project administration. **Jian Chen:** Conceptualization, Methodology, Software, Formal analysis, Data curation, Writing – original draft, Visualization. **Chun-Hung Yeh:** Conceptualization, Methodology, Software, Formal analysis, Writing – original draft. **Mark T Mackay:** Resources, Writing – review & editing, Project administration, Funding acquisition. **Yves d'Udekem:** Resources, Writing – review & editing, Supervision, Project administration, Funding acquisition. **David S Winlaw:** Resources, Writing – review & editing, Supervision, Project administration, Funding acquisition. **Ajay Iyengar:** Resources, Writing – review & editing. **Julian Ayer:** Investigation, Resources, Writing – review & editing. **Thomas L Gentles:** Resources, Writing – review & editing, Supervision, Project administration. **Rachael Cordina:** Conceptualization, Methodology, Software, Resources, Writing – original draft, Supervision, Project administration, Funding acquisition. **Joseph Y-M Yang:** Conceptualization, Methodology, Software, Formal analysis, Resources, Writing – original draft, Visualization, Supervision, Project administration.

Declaration of Competing Interest

The authors declare that they have no known competing financial interests or personal relationships that could have appeared to influence the work reported in this paper.

Data availability

The authors do not have permission to share data.

Acknowledgement

We would like to thank Derek Tran and Karina Laohachai for their contribution in the collection and curation of the cardiopulmonary exercise test data. This project was supported by a grant from the National Health and Medical Research Council (Project Grant 1047923) and a HeartKids Grants-in-Aid, The Royal Children's Hospital Foundation, Murdoch Children's Research Institute, The University of Melbourne, Department of Paediatrics, and the Victorian Government's Operational Infrastructure Support Program.

Appendix A. Supplementary data

Supplementary data to this article can be found online at https://doi.org/10.1016/j.nicl.2022.103151.

References

Alexander, A.L., Lee, J.E., Lazar, M., Field, A.S., 2007. Diffusion tensor imaging of the brain. Neurotherapeutics. 4 (3), 316–329. https://doi.org/10.1016/j.nurt.2007.05.011.

Andersson, J.L.R., Sotiropoulos, S.N., 2016. An integrated approach to correction for off-resonance effects and subject movement in diffusion MR imaging. NeuroImage. 125, 1063–1078. https://doi.org/10.1016/j.neuroimage.2015.10.019.

Andersson, J.L.R., Skare, S., Ashburner, J., 2003. How to correct susceptibility distortions in spin-echo echo-planar images: application to diffusion tensor imaging. NeuroImage. 20 (2), 870–888. https://doi.org/10.1016/S1053-8119(03)00336-7.

Bagge, C.N., Henderson, V.W., Laursen, H.B., Adelborg, K., Olsen, M., Madsen, N.L., 2018. Risk of dementia in adults with congenital heart disease: Population-based cohort study. Circulation 137 (18), 1912–1920. https://doi.org/10.1161/CIRCULATIONAHA.117.029686.

Barbeau, E.B., Descoteaux, M., Petrides, M., 2020. Dissociating the white matter tracts connecting the temporo-parietal cortical region with frontal cortex using diffusion tractography. Sci. Rep. 10 (1), 8186. https://doi.org/10.1038/s41598-020-64124-y.

Basser, P.J., Mattiello, J., LeBihan, D., 1994. MR diffusion tensor spectroscopy and imaging. Biophys. J . 66 (1), 259–267. https://doi.org/10.1016/s0006-3495(94)80775-1.

Basser, P.J., Mattiello, J., Lebihan, D., 1994. Estimation of the effective self-diffusion tensor from the NMR spin echo. J. Magn. Reson. B. 103 (3), 247–254. https://doi.org/10.1006/jmrb.1994.1037.

Bellinger, D.C., Watson, C.G., Rivkin, M.J., Robertson, R.L., Roberts, A.E., Stopp, C., Dunbar-Masterson, C., Bernson, D., DeMaso, D.R., Wypij, D., Newburger, J.W., 2015. Neuropsychological status and structural brain imaging in adolescents with single ventricle who underwent the Fontan procedure. J. Am. Heart Assoc. 4 (12), e002302. https://doi.org/10.1161/JAHA.115.002302.

Bhushan, C., Haldar, J.P., Choi, S., Joshi, A.A., Shattuck, D.W., Leahy, R.M., 2015. Co-registration and distortion correction of diffusion and anatomical images based on inverse contrast normalization. NeuroImage. 115, 269–280. https://doi.org/10.1016/j.neuroimage.2015.03.050.

Brewster, R.C., King, T.Z., Burns, T.G., Drossner, D.M., Mahle, W.T., 2015. White matter integrity dissociates verbal memory and auditory attention span in emerging adults with congenital heart disease. J. Int. Neuropsychol. Soc. 21 (1), 22–33. https://doi.org/10.1017/s135561771400109x.

Bucholz, E.M., Sleeper, L.A., Sananes, R., Brosig, C.L., Goldberg, C.S., Pasquali, S.K., Newburger, J.W., 2021. Trajectories in neurodevelopmental, health-related quality of life, and functional status outcomes by socioeconomic status and maternal education in children with single ventricle heart disease. J. Pediatr. 229, 289–293.e3.

Cabrera-Mino, C., Roy, B., Woo, M.A., Singh, S., Moye, S., Halnon, N.J., Lewis, A.B., Kumar, R., Pike, N.A., 2020. Reduced brain mammillary body volumes and memory deficits in adolescents who have undergone the Fontan procedure. Pediatr. Res. 87 (1), 169–175.

Cassidy, A.R., White, M.T., DeMaso, D.R., Newburger, J.W., Bellinger, D.C., 2015. Executive function in children and adolescents with critical cyanotic congenital heart disease. J. Int. Neuropsychol. Soc. 21 (1), 34–49. https://doi.org/10.1017/s1355617714001027.

Cayre, M., Falque, M., Mercier, O., Magalon, K., Durbec, P., 2021 Apr. Myelin repair: from animal models to humans. Front. Cell. Neurosci. 14 (15), 604865 https://doi.org/10.3389/fncel.2021.604865.

Chiang, H.L., Hsu, Y.C., Shang, C.Y., Tseng, W.I., Gau, S.S., 2020. White matter endophenotype candidates for ADHD: a diffusion imaging tractography study with sibling design. Psychol. Med. 50 (7), 1203–1213. https://doi.org/10.1017/s0033291719001120.

Claessens, N.H.P., Algra, S.O., Ouwehand, T.L., Jansen, N.J.G., Schappin, R., Haas, F., Eijsermans, M.J.C., Vries, L.S., Benders, M.J.N.L., Moeskops, P., Išgum, I., Haastert, I.C., Groenendaal, F., Breur, J.M.P.J., 2018. Perioperative neonatal brain injury is associated with worse school-age neurodevelopment in children with critical congenital heart disease. Dev. Med. Child Neurol. 60 (10), 1052–1058.

Claessens, N.H.P., Khalili, N., Isgum, I., ter Heide, H., Steenhuis, T.J., Turk, E., Jansen, N.J.G., de Vries, L.S., Breur, J.M.P.J., de Heus, R., Benders, M.J.N.L., 2019. Brain and CSF volumes in fetuses and neonates with antenatal diagnosis of critical congenital heart disease: A longitudinal MRI study. AJNR Am. J. Neuroradiol. 40 (5), 885–891.

Concha, L., 2014. A macroscopic view of microstructure: using diffusion-weighted images to infer damage, repair, and plasticity of white matter. Neuroscience 276, 14–28. https://doi.org/10.1016/j.neuroscience.2013.09.004.

Cordina, R., Grieve, S., Barnett, M., Lagopoulos, J., Malitz, N., Celermajer, D.S., 2014. Brain volumetric, regional cortical thickness and radiographic findings in adults with cyanotic congenital heart disease. Neuroimage Clin. 4, 319–325. https://doi.org/10.1016/j.nicl.2013.12.011.

Cremers, L.G.M., de Groot, M., Hofman, A., Krestin, G.P., van der Lugt, A., Niessen, W.J., Vernooij, M.W., Ikram, M.A., 2016. Altered tract-specific white matter microstructure is related to poorer cognitive performance: The Rotterdam Study. Neurobiol. Aging 39, 108–117.

d'Udekem, Y., Iyengar, A.J., Galati, J.C., Forsdick, V., Weintraub, R.G., Wheaton, G.R., Bullock, A., Justo, R.N., Grigg, L.E., Sholler, G.F., Hope, S., Radford, D.J., Gentles, T. L., Celermajer, D.S., Winlaw, D.S., 2014. Redefining expectations of long-term survival after the Fontan procedure: Twenty-five years of follow-up from the entire population of Australia and New Zealand. Circulation 130 (11_suppl_1). https://doi.org/10.1161/circulationaha.113.007764.

Dhollander, T., Raffelt, D., Connelly, A., 2016. Unsupervised 3-tissue response function estimation from single-shell or multi-shell diffusion MR data without a co-registered T1 image. ISMRM Workshop on Breaking the Barriers of Diffusion MRI, Lisbon, Portugal.

Egbe, A.C., Khan, A.R., Ammash, N.M., Barbara, D.W., Oliver, W.C., Said, S.M., Akintoye, E., Warnes, C.A., Connolly, H.M., 2017. Predictors of procedural complications in adult Fontan patients undergoing non-cardiac procedures. Heart 103 (22), 1813–1820.

Ehrler, M., Latal, B., Kretschmar, O., von Rhein, M., O'Gorman, T.R., 2020. Altered frontal white matter microstructure is associated with working memory impairments in adolescents with congenital heart disease: A diffusion tensor imaging study. NeuroImage Clin. 25, 102123 https://doi.org/10.1016/j.nicl.2019.102123.

Ehrler, M., Schlosser, L., Brugger, P., Greutmann, M., Oxenius, A., Kottke, R., O'Gorman Tuura, R., Latal, B., 2021. Altered white matter microstructure is related to cognition in adults with congenital heart disease. Brain Commun. 3 (1) https://doi.org/10.1093/braincomms/fcaa224.

Fitzgerald, J., Johnson, K., Kehoe, E., Bokde, A.L.W., Garavan, H., Gallagher, L., McGrath, J., 2015. Disrupted functional connectivity in dorsal and ventral attention networks during attention orienting in autism spectrum disorders. Autism Res. 8 (2), 136–152.

Fortin, J.-P., Parker, D., Tunç, B., Watanabe, T., Elliott, M.A., Ruparel, K., Roalf, D.R., Satterthwaite, T.D., Gur, R.C., Gur, R.E., Schultz, R.T., Verma, R., Shinohara, R.T., 2017. Harmonization of multi-site diffusion tensor imaging data. NeuroImage. 161, 149–170.

Gibson, E.M., Geraghty, A.C., Monje, M., 2018. Bad wrap: Myelin and myelin plasticity in health and disease. Dev Neurobiol. 78 (2), 123–135. https://doi.org/10.1002/dneu.22541.

Groeschel, S., Tournier, J.D., Northam, G.B., Baldeweg, T., Wyatt, J., Vollmer, B., Connelly, A., 2014. Identification and interpretation of microstructural abnormalities in motor pathways in adolescents born preterm. Neuroimage. 87, 209–219. https://doi.org/10.1016/j.neuroimage.2013.10.034.

Hammers, D., Spurgeon, E., Ryan, K., Persad, C., Barbas, N., Heidebrink, J., Darby, D., Giordani, B., 2012. Validity of a brief computerized cognitive screening test in dementia. J. Geriatr. Psychiatry Neurol. 25 (2), 89–99.

Hansen, E., Poole, T.A., Nguyen, V., Lerner, M., Wigal, T., Shannon, K., Wigal, S.B., Batra, A.S., 2012. Prevalence of ADHD symptoms in patients with congenital heart disease. Pediatr. Int. 54 (6), 838–843.

Harvey, P.D., 2019. Domains of cognition and their assessment. Dialogues Clin. Neurosci. 21 (3), 227–237. https://doi.org/10.31887/DCNS.2019.21.3/pharvey.

Hatton, S.N., Huynh, K.H., Bonilha, L., Abela, E., Alhusaini, S., Altmann, A., Alvim, M.K. M., Balachandra, A.R., Bartolini, E., Bender, B., Bernasconi, N., Bernasconi, A., Bernhardt, B., Bargallo, N., Caldairou, B., Caligiuri, M.E., Carr, S.J.A., Cavalleri, G.L., Cendes, F., Concha, L., Davoodi-bojd, E., Desmond, P.M., Devinsky, O., Doherty, C. P., Domin, M., Duncan, J.S., Focke, N.K., Foley, S.F., Gambardella, A., Gleichgerrcht, E., Guerrini, R., Hamandi, K., Ishikawa, A., Keller, S.S., Kochunov, P. V., Kotikalapudi, R., Kreilkamp, B.A.K., Kwan, P., Labate, A., Langner, S., Lenge, M., Liu, M., Lui, E., Martin, P., Mascalchi, M., Moreira, J.C.V., Morita-Sherman, M.E., O'Brien, T.J., Pardoe, H.R., Pariente, J.C., Ribeiro, L.F., Richardson, M.P., Rocha, C. S., Rodríguez-Cruces, R., Rosenow, F., Severino, M., Sinclair, B., Soltanian-Zadeh, H., Striano, P., Taylor, P.N., Thomas, R.H., Tortora, D., Velakoulis, D., Vezzani, A., Vivash, L., von Podewils, F., Vos, S.B., Weber, B., Winston, G.P., Yasuda, C.L., Zhu, A.H., Thompson, P.M., Whelan, C.D., Jahanshad, N., Sisodiya, S.M., McDonald, C.R., 2020. White matter abnormalities across different epilepsy syndromes in adults: an ENIGMA-Epilepsy study. Brain. 143 (8), 2454–2473.

Heal, M.E., Jackson, L.B., Atz, A.M., Butts, R.J., 2017. Effects of persistent Fontan fenestration patency on cardiopulmonary exercise testing variables. Congenital Heart Disease. 12, 399–402. https://doi.org/10.1111/chd.12451.

Hoeft, F., Barnea-Goraly, N., Haas, B.W., Golarai, G., Ng, D., Mills, D., Korenberg, J., Bellugi, U., Galaburda, A., Reiss, A.L., 2007. More is not always better: increased fractional anisotropy of superior longitudinal fasciculus associated with poor visuospatial abilities in Williams syndrome. J. Neurosci. 27 (44), 11960–11965.

Huang, L., Wu, Z.-B., ZhuGe, Q., Zheng, W., Shao, B., Wang, B., Sun, F., Jin, K., 2014. Glial scar formation occurs in the human brain after ischemic stroke. Int. J. Med. Sci. 11 (4), 344–348.

Idorn, L., Jensen, A.S., Juul, K., Overgaard, D., Nielsen, N.P., Sørensen, K., Reimers, J.I., Søndergaard, L., 2013. Quality of life and cognitive function in Fontan patients, a population-based study. Int. J. Cardiol. 168 (4), 3230–3235.

Issar, P., Nehra, M., Singh, G., Issar, S.K., 2018. Conventional and advanced brain MR imaging in patients with sickle cell anemia. Indian J. Radiol. Imaging. 28 (3), 305–311. https://doi.org/10.4103/ijri.IJRI_166_17.

Jeurissen, B., Leemans, A., Tournier, J.D., Jones, D.K., Sijbers, J., 2013. Investigating the prevalence of complex fiber configurations in white matter tissue with diffusion magnetic resonance imaging. Hum. Brain Mapp. 34 (11), 2747–2766. https://doi.org/10.1002/hbm.22099.

Jeurissen, B., Tournier, J.D., Dhollander, T., Connelly, A., Sijbers, J., 2014. Multi-tissue constrained spherical deconvolution for improved analysis of multi-shell diffusion MRI data. NeuroImage. 103, 411–426. https://doi.org/10.1016/j.neuroimage.2014.07.061.

Jung, S., Kim, J.-H., Sung, G., Ko, Y.-G., Bang, M., Park, C.-I., Lee, S.-H., 2020. Uncinate fasciculus white matter connectivity related to impaired social perception and cross-sectional and longitudinal symptoms in patients with schizophrenia spectrum psychosis. Neurosci. Lett. 737, 135144.

Kellner, E., Dhital, B., Kiselev, V.G., Reisert, M., 2016. Gibbs-ringing artifact removal based on local subvoxel-shifts: Gibbs-Ringing Artifact Removal. Gibbs-ringing artifact removal based on local subvoxel-shifts. 76 (5), 1574–1581.

Kelly, C.J., Christiaens, D., Batalle, D., Makropoulos, A., Cordero-Grande, L., Steinweg, J. K., O'Muircheartaigh, J., Khan, H., Lee, G., Victor, S., Alexander, D.C., Zhang, H., Simpson, J., Hajnal, J.V., Edwards, A.D., Rutherford, M.A., Counsell, S.J., 2019. Abnormal microstructural development of the cerebral cortex in neonates with congenital heart disease is associated with impaired cerebral oxygen delivery. J. Am. Heart Assoc. 8 (5) https://doi.org/10.1161/JAHA.118.009893.

Kim, S.E., Jung, S., Sung, G., Bang, M., Lee, S.-H., 2021. Impaired cerebro-cerebellar white matter connectivity and its associations with cognitive function in patients with schizophrenia. npj Schizophr. 7 (1), 38. https://doi.org/10.1038/s41537-021-00169-w.

Klouda, L., Franklin, W.J., Saraf, A., Parekh, D.R., Schwartz, D.D., 2017. Neurocognitive and executive functioning in adult survivors of congenital heart disease. Congenit Heart Dis. 12 (1), 91–98. https://doi.org/10.1111/chd.12409.

Lee, F.-T., Seed, M., Sun, L., Marini, D., 2021. Fetal brain issues in congenital heart disease. Transl. Pediatr. 10 (8), 2182–2196. https://doi.org/10.21037/tp-20-224.

Lemler, M.S., Scott, W.A., Leonard, S.R., Stromberg, D., Ramaciotti, C., 2002. Fenestration improves clinical outcome of the Fontan procedure. Circulation 105 (2), 207–212. https://doi.org/10.1161/hc0202.102237.

Limperopoulos, C., Tworetzky, W., McElhinney, D.B., Newburger, J.W., Brown, D.W., Robertson, R.L., Guizard, N., McGrath, E., Geva, J., Annese, D., Dunbar-Masterson, C., Trainor, B., Laussen, P.C., du Plessis, A.J., 2010. Brain volume and metabolism in fetuses with congenital heart disease: evaluation with quantitative magnetic resonance imaging and spectroscopy. Circulation 121 (1), 26–33.

Marelli, A., Miller, S.P., Marino, B.S., Jefferson, A.L., Newburger, J.W., 2016. Brain in congenital heart disease across the lifespan: The cumulative burden of injury. Circulation 133 (20), 1951–1962. https://doi.org/10.1161/circulationaha.115.019881.

Martinez Sosa, S., Smith, K.J., 2017 Oct 12. Understanding a role for hypoxia in lesion formation and location in the deep and periventricular white matter in small vessel disease and multiple sclerosis. Clin. Sci. (Lond). 131 (20), 2503–2524. https://doi.org/10.1042/CS20170981.

Maruff, P., Thomas, E., Cysique, L., Brew, B., Collie, A., Snyder, P., Pietrzak, R.H., 2009. Validity of the CogState brief battery: Relationship to standardized tests and sensitivity to cognitive impairment in mild traumatic brain injury, schizophrenia, and AIDS dementia complex. Arch. Clin. Neuropsychol. 24 (2), 165–178.

McKenna, B.S., Theilmann, R.J., Sutherland, A.N., Eyler, L.T., 2015. Fusing functional MRI and diffusion tensor imaging measures of brain function and structure to predict working memory and processing speed performance among inter-episode bipolar patients. J. Int. Neuropsychol. Soc. 21 (5), 330–341. https://doi.org/10.1017/S1355617715000314.

Mills, R., McCusker, C.G., Tennyson, C., Hanna, D., 2018. Neuropsychological outcomes in CHD beyond childhood: a meta-analysis. Cardiol. Young 28 (3), 421–431. https://doi.org/10.1017/s104795111700230x.

Morton, P.D., Ishibashi, N., Jonas, R.A., 2017. Neurodevelopmental abnormalities and congenital heart disease: Insights into altered brain maturation. Circ. Res. 120 (6), 960–977. https://doi.org/10.1161/CIRCRESAHA.116.309048.

Naef, N., Schlosser, L., Brugger, P., Greutmann, M., Oxenius, A., Wehrle, F., Kottke, R., Latal, B., O'Gorman, R.T., 2021. Brain volumes in adults with congenital heart disease correlate with executive function abilities. Brain Imaging Behav. 15 (5), 2308–2316.

Nakajima, R., Kinoshita, M., Shinohara, H., Nakada, M., 2020. The superior longitudinal fascicle: reconsidering the fronto-parietal neural network based on anatomy and function. Brain Imaging Behav. 14 (6), 2817–2830. https://doi.org/10.1007/s11682-019-00187-4.

Newburger, J.W., Wypij, D., Bellinger, D.C., du Plessis, A.J., Kuban, K.C.K., Rappaport, L. A., Almirall, D., Wessel, D.L., Jonas, R.A., Wernovsky, G., 2003. Length of stay after infant heart surgery is related to cognitive outcome at age 8 years. J. Pediatr. 143 (1), 67–73.

Ohuchi, H., 2017. Where is the "optimal" Fontan hemodynamics? Korean Circ J. 47 (6), 842–857. https://doi.org/10.4070/kcj.2017.0105.

Oschwald, J., Mérillat, S., Liem, F., Röcke, C., Martin, M., Jäncke, L., 2019. Lagged coupled changes between white matter microstructure and processing speed in healthy aging: A longitudinal investigation. Front. Aging Neurosci. 11, 298. https://doi.org/10.3389/fnagi.2019.00298.

Owen, M., Shevell, M., Majnemer, A., Limperopoulos, C., 2011. Abnormal brain structure and function in newborns with complex congenital heart defects before open heart surgery: A review of the evidence. J. Child Neurol. 26 (6), 743–755. https://doi.org/10.1177/0883073811402073.

Penke, L., Maniega, S.M., Murray, C., Gow, A.J., Valdes Hernandez, M.C., Clayden, J.D., Starr, J.M., Wardlaw, J.M., Bastin, M.E., Deary, I.J., 2010. A general factor of brain white matter integrity predicts information processing speed in healthy older people. J. Neurosci. 30 (22), 7569–7574.

Plappert, L., Edwards, S., Senatore, A., De Martini, A., 2022. The epidemiology of persons living with Fontan in 2020 and projections for 2030: Development of an epidemiology model providing multinational estimates. Adv. Ther. 39 (2), 1004–1015. https://doi.org/10.1007/s12325-021-02002-3.

Raffelt, D.A., Tournier, J.D., Smith, R.E., Vaughan, D.N., Jackson, G., Ridgway, G.R., et al., 2017. Investigating white matter fibre density and morphology using fixel-based analysis. NeuroImage. 144 (Pt A), 58–73. https://doi.org/10.1016/j.neuroimage.2016.09.029.

Rajagopalan, V., Votava-Smith, J.K., Zhuang, X., Brian, J., Marshall, L., Panigrahy, A., Paquette, L., 2018. Fetuses with single ventricle congenital heart disease manifest impairment of regional brain growth. Prenat. Diagn. 38 (13), 1042–1048.

Reuter-Lorenz, P.A., Park, D.C., 2014. How does it STAC up? Revisiting the scaffolding theory of aging and cognition. Neuropsychol. Rev. 24 (3), 355–370. https://doi.org/10.1007/s11065-014-9270-9.

Rivkin MJ, Watson CG, Scoppettuolo LA, Wypij D, Vajapeyam S, Bellinger DC, et al. Adolescents with D-transposition of the great arteries repaired in early infancy demonstrate reduced white matter microstructure associated with clinical risk factors. J Thorac Cardiovasc Surg. 2013;146(3):543-9.e1. DOI: 10.1016/j.jtcvs.2012.12.006.

Rollins CK, Watson CG, Asaro LA, Wypij D, Vajapeyam S, Bellinger DC, et al. White matter microstructure and cognition in adolescents with congenital heart disease. J Pediatr. 2014;165(5):936-44.e1-2. DOI: 10.1016/j.jpeds.2014.07.028.

Sadhwani, A., Wypij, D., Rofeberg, V., Gholipour, A., Mittleman, M., Rohde, J., Velasco-Annis, C., Calderon, J., Friedman, K.G., Tworetzky, W., Grant, P.E., Soul, J.S., Warfield, S.K., Newburger, J.W., Ortinau, C.M., Rollins, C.K., 2022. Fetal brain volume predicts neurodevelopment in congenital heart disease. Circulation 145 (15), 1108–1119.

Sasson, E., Doniger, G.M., Pasternak, O., Tarrasch, R., Assaf, Y., 2013;7:32-. White matter correlates of cognitive domains in normal aging with diffusion tensor imaging. Front. Neurosci. https://doi.org/10.3389/fnins.2013.00032.

Sattler, C., Toro, P., Schönknecht, P., Schröder, J., 2012. Cognitive activity, education and socioeconomic status as preventive factors for mild cognitive impairment and Alzheimer's disease. Psychiatry Res. 196 (1), 90–95. https://doi.org/10.1016/j.psychres.2011.11.012.

Schafstedde, M., Nordmeyer, S., Schleiger, A., Nordmeyer, J., Berger, F., Kramer, P., et al., 2021. Persisting and reoccurring cyanosis after Fontan operation is associated with increased late mortality. Eur. J. Cardiothorac. Surg. 61 (1), 54–61. https://doi.org/10.1093/ejcts/ezab298.

Schilling, K.G., Rheault, F., Petit, L., Hansen, C.B., Nath, V., Yeh, F.-C., Girard, G., Barakovic, M., Rafael-Patino, J., Yu, T., Fischi-Gomez, E., Pizzolato, M., Ocampo-Pineda, M., Schiavi, S., Canales-Rodríguez, E.J., Daducci, A., Granziera, C., Innocenti, G., Thiran, J.-P., Mancini, L., Wastling, S., Cocozza, S., Petracca, M., Pontillo, G., Mancini, M., Vos, S.B., Vakharia, V.N., Duncan, J.S., Melero, H., Manzanedo, L., Sanz-Morales, E., Peña-Melián, Á., Calamante, F., Attyé, A., Cabeen, R.P., Korobova, L., Toga, A.W., Vijayakumari, A.A., Parker, D., Verma, R., Radwan, A., Sunaert, S., Emsell, L., De Luca, A., Leemans, A., Bajada, C.J., Haroon, H., Azadbakht, H., Chamberland, M., Genc, S., Tax, C.M.W., Yeh, P.-H., Srikanchana, R., Mcknight, C.D., Yang, J.-M., Chen, J., Kelly, C.E., Yeh, C.-H., Cochereau, J., Maller, J.J., Welton, T., Almairac, F., Seunarine, K.K., Clark, C.A., Zhang, F., Makris, N., Golby, A., Rathi, Y., O'Donnell, L.J., Xia, Y., Aydogan, D.B., Shi, Y., Fernandes, F.G., Raemaekers, M., Warrington, S., Michielse, S., Ramírez-Manzanares, A., Concha, L., Aranda, R., Meraz, M.R., Lerma-Usabiaga, G., Roitman, L., Fekonja, L.S., Calarco, N., Joseph, M., Nakua, H., Voineskos, A.N., Karan, P., Grenier, G., Legarreta, J.H., Adluru, N., Nair, V.A., Prabhakaran, V., Alexander, A.L., Kamagata, K., Saito, Y., Uchida, W., Andica, C., Abe, M., Bayrak, R.G., Wheeler-Kingshott, C.A.M.G., D'Angelo, E., Palesi, F., Savini, G., Rolandi, N., Guevara, P., Houenou, J., López-López, N., Mangin, J.-F., Poupon, C., Román, C., Vázquez, A., Maffei, C., Arantes, M., Andrade, J.P., Silva, S.M., Calhoun, V.D., Caverzasi, E., Sacco, S., Lauricella, M., Pestilli, F., Bullock, D., Zhan, Y., Brignoni-Perez, E., Lebel, C., Reynolds, J.E., Nestrasil, I., Labounek, R., Lenglet, C., Paulson, A., Aulicka, S., Heilbronner, S.R., Heuer, K., Chandio, B.Q., Guaje, J., Tang, W., Garyfallidis, E., Raja, R., Anderson, A.W., Landman, B.A., Descoteaux, M., 2021. Tractography dissection variability: What happens when 42 groups dissect 14 white matter bundles on the same dataset? NeuroImage. 243, 118502.

Singh, S., Roy, B., Pike, N., Daniel, E., Ehlert, L., Lewis, A.B., Halnon, N., Woo, M.A., Kumar, R., 2019. Altered brain diffusion tensor imaging indices in adolescents with the Fontan palliation. Neuroradiology 61 (7), 811–824.

Smith, R., Raffelt, D., Tournier, J.-D., Connelly, A., 2020. Quantitative streamlines tractography: methods and inter-subject normalisation. https://doi.org/10.31219/osf.io/c67kn.

Spaeder, M.C., Klugman, D., Skurow-Todd, K., Glass, P., Jonas, R.A., Donofrio, M.T., 2017. Perioperative near-infrared spectroscopy monitoring in neonates with congenital heart disease: Relationship of cerebral tissue oxygenation index variability with neurodevelopmental outcome. Pediatr. Crit. Care Med. 18 (3), 213–218. https://doi.org/10.1097/pcc.0000000000001056.

Sun, L., Macgowan, C.K., Sled, J.G., Yoo, S.-J., Manlhiot, C., Porayette, P., Grosse-Wortmann, L., Jaeggi, E., McCrindle, B.W., Kingdom, J., Hickey, E., Miller, S., Seed, M., 2015. Reduced fetal cerebral oxygen consumption is associated with smaller brain size in fetuses with congenital heart disease. Circulation 131 (15), 1313–1323.

Tamnes, C.K., Agartz, I., 2016. White matter microstructure in early-onset schizophrenia: A systematic review of diffusion tensor imaging studies. J. Am. Acad. Child Adolesc. Psychiatry 55 (4), 269–279. https://doi.org/10.1016/j.jaac.2016.01.004.

Tournier, J.D., Mori, S., Leemans, A., 2011. Diffusion tensor imaging and beyond. Magn. Reson. Med. 65 (6), 1532–1556. https://doi.org/10.1002/mrm.22924.

Tournier, J.-D., Smith, R., Raffelt, D., Tabbara, R., Dhollander, T., Pietsch, M., Christiaens, D., Jeurissen, B., Yeh, C.-H., Connelly, A., 2019. MRtrix3: A fast, flexible and open software framework for medical image processing and visualisation. NeuroImage. 202, 116137.

Tran, D.L., Gibson, H., Maiorana, A.J., Verrall, C.E., Baker, D.W., Clode, M., Lubans, D.R., Zannino, D., Bullock, A., Ferrie, S., Briody, J., Simm, P., Wijesekera, V., D'Almeida, M., Gosbell, S.E., Davis, G.M., Weintraub, R., Keech, A.C., Puranik, R., Ugander, M., Justo, R., Zentner, D., Majumdar, A., Grigg, L., Coombes, J.S., d'Udekem, Y., Morris, N.R., Ayer, J., Celermajer, D.S., Cordina, R., 2022. Exercise intolerance, benefits, and prescription for people living with a fontan circulation: the fontan fitness intervention trial (F-FIT) - rationale and design. Front. Pediatr. 9, 799125 https://doi.org/10.3389/fped.2021.799125.

Tuch, D.S., Reese, T.G., Wiegell, M.R., Makris, N., Belliveau, J.W., Wedeen, V.J., 2002. High angular resolution diffusion imaging reveals intravoxel white matter fiber heterogeneity. Magn. Reson. Med. 48 (4), 577–582. https://doi.org/10.1002/mrm.10268.

Tustison, N.J., Avants, B.B., Cook, P.A., Zheng, Y., Egan, A., Yushkevich, P.A., et al., 2010. N4ITK: improved N3 bias correction. IEEE Trans. Med. Imaging 29 (6), 1310–1320. https://doi.org/10.1109/tmi.2010.2046908.

Veraart, J., Sijbers, J., Sunaert, S., Leemans, A., Jeurissen, B., 2013. Weighted linear least squares estimation of diffusion MRI parameters: strengths, limitations, and pitfalls. NeuroImage. 81, 335–346. https://doi.org/10.1016/j.neuroimage.2013.05.028.

Veraart, J., Fieremans, E., Novikov, D.S., 2016. Diffusion MRI noise mapping using random matrix theory. Magn. Reson. Med. 76 (5), 1582–1593. https://doi.org/10.1002/mrm.26059.

Verrall, C.E., Blue, G.M., Loughran-Fowlds, A., Kasparian, N., Gecz, J., Walker, K., Dunwoodie, S.L., Cordina, R., Sholler, G., Badawi, N., Winlaw, D., 2019. 'Big issues' in neurodevelopment for children and adults with congenital heart disease. Open Heart 6 (2), e000998.

Verrall, C.E., Yang, J.Y.M., Chen, J., Schembri, A., d'Udekem, Y., Zannino, D., Kasparian, N.A., du Plessis, K., Grieve, S.M., Welton, T., Barton, B., Gentles, T.L., Celermajer, D.S., Attard, C., Rice, K., Ayer, J., Mandelstam, S., Winlaw, D.S., Mackay, M.T., Cordina, R., 2021. Neurocognitive dysfunction and smaller brain volumes in adolescents and adults with a Fontan circulation. Circulation 143 (9), 878–891.

Villalón-Reina, J.E., Martínez, K., Qu, X., Ching, C.R.K., Nir, T.M., Kothapalli, D., Corbin, C., Sun, D., Lin, A., Forsyth, J.K., Kushan, L., Vajdi, A., Jalbrzikowski, M., Hansen, L., Jonas, R.K., van Amelsvoort, T., Bakker, G., Kates, W.R., Antshel, K.M., Fremont, W., Campbell, L.E., McCabe, K.L., Daly, E., Gudbrandsen, M., Murphy, C.M., Murphy, D., Craig, M., Emanuel, B., McDonald-McGinn, D.M., Vorstman, J.A.S., Fiksinski, A.M., Koops, S., Ruparel, K., Roalf, D., Gur, R.E., Eric Schmitt, J., Simon, T.J., Goodrich-Hunsaker, N.J., Durdle, C.A., Doherty, J.L., Cunningham, A.C., van den Bree, M., Linden, D.E.J., Owen, M., Moss, H., Kelly, S., Donohoe, G., Murphy, K.C., Arango, C., Jahanshad, N., Thompson, P.M., Bearden, C.E., 2020. Altered white matter microstructure in 22q11.2 deletion syndrome: a multisite diffusion tensor imaging study. Mol. Psychiatry 25 (11), 2818–2831.

von Rhein, M., Buchmann, A., Hagmann, C., Huber, R., Klaver, P., Knirsch, W., et al., 2014. Brain volumes predict neurodevelopment in adolescents after surgery for congenital heart disease. Brain. 137 (1), 268–276. https://doi.org/10.1093/brain/awt322 %J Brain.

Wasserthal, J., Neher, P., Maier-Hein, K.H., 2018. TractSeg - Fast and accurate white matter tract segmentation. NeuroImage. 183, 239–253. https://doi.org/10.1016/j.neuroimage.2018.07.070.

Watson CG, Stopp C, Wypij D, Bellinger DC, Newburger JW, Rivkin MJ. Altered white matter microstructure correlates with IQ and processing speed in children and adolescents post-Fontan. J Pediatr. 2018;200:140-9.e4 DOI: 10.1016/j.jpeds.2018.04.022.

Witelson, S.F., 1989. Hand and sex differences in the isthmus and genu of the human corpus callosum. A postmortem morphological study. Brain. 112 (Pt 3), 799–835. https://doi.org/10.1093/brain/112.3.799.

Yang, J.-M., Yeh, C.-H., Poupon, C., Calamante, F., 2021. Diffusion MRI tractography for neurosurgery: the basics, current state, technical reliability and challenges. Phys. Med. Biol. 66 (15), 15TR01.

Yeh, C.-H., Jones, D.K., Liang, X., Descoteaux, M., Connelly, A., 2021. Mapping structural connectivity using diffusion MRI: challenges and opportunities. J. Magn. Reson. Imaging 53 (6), 1666–1682. https://doi.org/10.1002/jmri.27188.

Zaidi, A.H., Newburger, J.W., Wypij, D., Stopp, C., Watson, C.G., Friedman, K.G., Rivkin, M.J., Rollins, C.K., 2018. Ascending aorta size at birth predicts white matter microstructure in adolescents who underwent Fontan palliation. J Am Heart Assoc. 7 (24), e010395. https://doi.org/10.1161/jaha.118.010395.

Zentner, D., Celermajer, D.S., Gentles, T., d'Udekem, Y., Ayer, J., Blue, G.M., Bridgman, C., Burchill, L., Cheung, M., Cordina, R., Culnane, E., Davis, A., du Plessis, K., Eagleson, K., Finucane, K., Frank, B., Greenway, S., Grigg, L., Hardikar, W., Hornung, T., Hynson, J., Iyengar, A.J., James, P., Justo, R., Kalman, J., Kasparian, N., Le, B., Marshall, K., Mathew, J., McGiffin, D., McGuire, M., Monagle, P., Moore, B., Neilsen, J., O'Connor, B., O'Donnell, C., Pflaumer, A., Rice, K., Sholler, G., Skinner, J.R., Sood, S., Ward, J., Weintraub, R., Wilson, T., Wilson, W., Winlaw, D., Wood, A., 2020. Management of people with a Fontan circulation: a Cardiac Society of Australia and New Zealand position statement. Heart, Lung Circ. 29 (1), 5–39.